



# Lineshape of the singlet-triplet excitations in the dimer system $\text{Sr}_3\text{Cr}_2\text{O}_8$ to first order in the high-density $1/z$ expansion

J. Jensen

*Niels Bohr Institute, Universitetsparken 5, DK-2100 Copenhagen, Denmark*

D. L. Quintero-Castro and A. T. M. N. Islam

*Helmholtz-Zentrum Berlin für Materialien und Energie, D-14109 Berlin, Germany*

K. C. Rule

*Helmholtz-Zentrum Berlin für Materialien und Energie, D-14109 Berlin, Germany**and The Bragg Institute, ANSTO, Kirrawee DC NSW 2234, Australia*

M. Månsson

*Laboratory for Neutron Scattering, Paul Scherrer Institut, CH-5232 Villigen PSI, Switzerland**and Laboratory for Quantum Magnetism (LQM), École Polytechnique Fédérale de Lausanne (EPFL), CH-1015 Lausanne, Switzerland*

B. Lake

*Helmholtz-Zentrum Berlin für Materialien und Energie, D-14109 Berlin, Germany  
and Institut für Festkörperphysik, Technische Universität Berlin, D-10623 Berlin, Germany*

(Received 10 March 2014; published 11 April 2014)

The  $\text{Cr}^{5+}$  ions in  $\text{Sr}_3\text{Cr}_2\text{O}_8$  constitute a strongly correlated spin-1/2 dimer system. Experiments show that the collective singlet-triplet excitations in this system are well defined in the zero-temperature limit, but, when heated, the inelastic neutron scattering peaks decrease rapidly in intensity and acquire a nonzero line width. When including the fluctuations to leading order in  $1/z$ , where  $z$  is the coordination number, the diagrammatic high-density expansion is found to offer an accurate description of the singlet-triplet excitations. The theory explains not only the temperature dependencies of the intensities and line widths, but also that strong correlation causes the lineshapes to become asymmetric at temperatures comparable to the excitation energies.

DOI: [10.1103/PhysRevB.89.134407](https://doi.org/10.1103/PhysRevB.89.134407)

PACS number(s): 75.10.-b, 75.30.-m, 67.85.Jk

## I. INTRODUCTION

In certain magnetic compounds, strong antiferromagnetic interactions couple the spins into pairs, forming dimers. The energy levels in this kind of system consist of a singlet ground state and triplet excited states. The dimers can interact with their neighbors via weaker interdimer interactions, making the excitations dispersive with a finite bandwidth and a gap. The dimer excitations are hard-core bosons since they are not able to propagate via a dimer which is already in an excited state. These excitations are similar to crystal-field excitations in rare-earth systems [1], and in contrast to bosonic excitations like phonons or spin waves, the crystal-field or the dimer excitations are strongly scattered by local thermal variations. In the zero-temperature limit the line widths of these dimer excitations are small compared to the experimental resolution but at finite temperatures, when the energies of the thermal fluctuations and the excitations become comparable, the line widths broaden asymmetrically [2].

This is the situation for the three-dimensional dimer system  $\text{Sr}_3\text{Cr}_2\text{O}_8$ . It consists of hexagonal bilayers of  $\text{Cr}^{5+}$  ions stacked along the  $c$  axis as shown in the inset in Fig. 1. The magnetic interaction  $J_0$  between first neighbors is one order of magnitude stronger than any other interaction, and the pairs of  $\text{Cr}^{5+}$  ions with spin  $S = 1/2$  become well-defined dimers. Previous work has shown that the interactions between the dimers imply that the local singlet-triplet excitations become propagating collective modes, which disperse in all directions

in reciprocal space due to the three-dimensional nature of the interdimer interactions [2,3]. The asymmetric broadening of the scattering peaks is not unique to  $\text{Sr}_3\text{Cr}_2\text{O}_8$ . Inelastic neutron scattering experiments using the time of flight technique and the high resolution neutron resonance spin-echo method have shown similar broadenings in the one-dimensional dimer Heisenberg chain compound  $[\text{Cu}(\text{NO}_3)_2 \cdot 2.5(\text{D}_2\text{O})]$  [4,5].

An understanding of the asymmetric lineshape might possibly be achieved by mapping the spin excitations onto a model of interacting bosons where an infinite on-site repulsion between the triplet excitations is used to model the hard-core constraint [6,7]. Here we are going to utilize a more systematic approach based on the diagrammatic, high-density expansion of the correlation functions, which was developed by Stinchcombe [8] based on the work by Vaks *et al.* [9]. To zero order in  $1/z$ , the expansion generates the mean-field/random phase approximation (MF/RPA). The leading order effects due to fluctuations appear in the order  $(1/z)^1$ , where  $z$  is the coordination number. The spatial variation in the thermal population of the different levels of the single units (dimers) acts like time-dependent impurities, and it is possible to construct an effective fluctuating medium, common for all sites, like the one introduced in the coherent-potential approximation for the case of a static distribution of impurities [1,10]. This self-consistent, effective medium version of the theory to first order in  $1/z$  has previously been developed and applied to singlet-singlet [1,11,12] and singlet-doublet

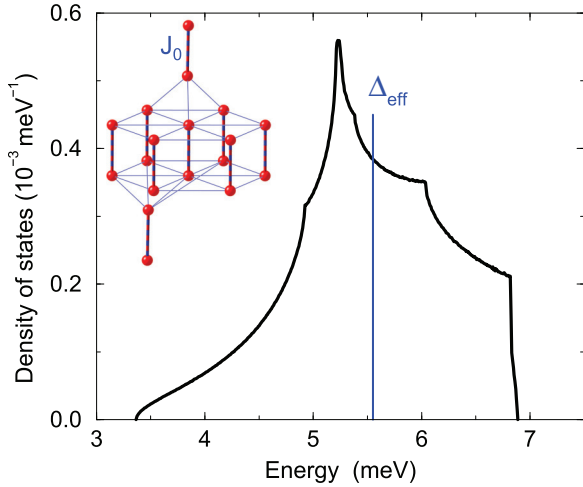


FIG. 1. (Color online) The density of states of singlet-triplet excitations in  $\text{Sr}_3\text{Cr}_2\text{O}_8$  in the zero temperature limit. It is determined from the RPA model in Ref. [3] as an average over the three twinned domains. The inset shows the spin-dimer structure in  $\text{Sr}_3\text{Cr}_2\text{O}_8$ . The dimer units are the  $\text{Cr}^{5+}$  pairs of nearest neighbors connected by the blue-red vertical bonds, and the intradimer exchange interaction is denoted by  $J_0 = \Delta$ . A detailed description of the magnetic exchange interactions in  $\text{Sr}_3\text{Cr}_2\text{O}_8$  can be found in Ref. [3].

[1,10,13] systems, and recently the theory was extended to the present case of a singlet-triplet system and applied to  $\text{TlCuCl}_3$  [14]. In the present paper the predictions of this theory are compared with the results of a comprehensive experimental investigation of the singlet-triplet excitations in the  $\text{Sr}_3\text{Cr}_2\text{O}_8$  dimer system. We shall emphasize that, when utilizing the (effective) MF/RPA model parameters derived previously for the system [2,3], there are no free parameters left for the present advancements in the description of the singlet-triplet excitations in  $\text{Sr}_3\text{Cr}_2\text{O}_8$ .

## II. EXPERIMENTAL DETAILS AND SAMPLE DETAILS

The crystal structure of  $\text{Sr}_3\text{Cr}_2\text{O}_8$  is trigonal at room temperature and belongs to the space group  $R\bar{3}m$  making the compound magnetically frustrated at these temperatures. However, it undergoes a Jahn-Teller distortion at 285 K that lifts the degeneracy of the singly occupied  $e$  orbitals of  $\text{Cr}^{5+}$  and hence lowers the frustration. The low-temperature structure is monoclinic ( $C2/c$ ) and is stable below 120 K [15–17]. The monoclinic structure gives rise to three crystal twins of similar volumes, which are rotated with respect to each other. Each of these twins produces a separate excitation branch; these excitation branches coincide at the  $\Gamma$  point but are nondegenerate elsewhere. The hexagonal notation is in use throughout the manuscript.

Single crystal samples of  $\text{Sr}_3\text{Cr}_2\text{O}_8$  were grown using the floating zone technique [18]. The temperature dependence of the lineshapes of the magnetic excitations was investigated by means of inelastic neutron scattering using two triple axis spectrometers, V2-FLEX at the Helmholtz Zentrum Berlin and TASP at the Paul Scherrer Institute. Two single crystals of total mass 7.745 g were coaligned and used for the experiment on V2-FLEX and only one crystal of mass 3.69 g was measured

on TASP. Constant wave-vector scans at different temperatures were performed at  $(0.5, 0.5, 3)$  with a final wave number  $k_f = 1.2$ , at  $(0, 0, 7.5)$  with  $k_f = 1.1$ , and at  $(0, 0, 3)$  with  $k_f = 1.55 \text{ \AA}^{-1}$ .

## III. THE $1/z$ EXPANSION THEORY

The influence of fluctuations on the magnetic properties are analyzed by performing a systematic high-density expansion [8] of the two-site Green's function, i.e., of the  $\tau$ -ordered ensemble average

$$G^{\alpha\beta}(ij, \tau_1 - \tau_2) = -\langle T_\tau S_{i\alpha}(\tau_1) S_{j\beta}(\tau_2) \rangle, \quad (1)$$

where  $T_\tau$  is the  $\tau$  ordering operator and  $S_{i\alpha}$  is the  $\alpha$ th component of the (effective) spin variable at site  $i$ . To zeroth order, the fluctuations are neglected and the theory is identical with the RPA theory. To first order, the theory includes the effects of the fluctuations in the surroundings of each single site. These single-site fluctuations may be accounted for in a self-consistent manner, since the fluctuating surroundings, to first order in  $1/z$ , constitute an “effective medium” common for every single site [1,10]. The Fourier transform of Green's function is  $G^{\alpha\beta}(\vec{q}, i\omega_n)$ , where  $\omega_n = 2\pi n k T / \hbar$  is the Matsubara frequency, in terms of which the single-site Green's function is

$$G^{\alpha\beta}(i\omega_n) \equiv G^{\alpha\beta}(jj, i\omega_n) = \frac{1}{N} \sum_{\vec{q}} G^{\alpha\beta}(\vec{q}, i\omega_n). \quad (2)$$

Assuming a diagonal set of final Green's functions  $G_p(\vec{q}, i\omega_n)$  (see Ref. [14]), they are determined self-consistently in terms of the effective-medium couplings  $K_p(i\omega_n)$ :

$$G_p(\vec{q}, i\omega_n) = \frac{G_p(i\omega_n)}{1 + \{J(\vec{q}) - K_p(i\omega_n)\} G_p(i\omega_n)}, \quad (3)$$

where  $J(\vec{q})$  is the Fourier transform of the total two-ion coupling, and

$$K_p(i\omega_n) = \frac{1}{N} \sum_{\vec{q}} J(\vec{q}) \frac{G_p(\vec{q}, i\omega_n)}{G_p(i\omega_n)} \quad (4)$$

is the sum of all chain diagrams, which start and end at the same site without crossing this site in between. The single-site Green's functions crossing themselves,  $G_p(i\omega_n)$ , are determined by Dyson equations which, in the order  $1/z$ , include the second and fourth order cumulants. This calculation has been carried through in the singlet-triplet case in Ref. [14]. The single-site dynamics are determined by the coupling  $K_p(i\omega_n)$  to the surrounding effective medium, which, in turn, determines the properties of the effective medium.

To first order in  $1/z$  the theory predicts perfectly well-defined excitations in the zero temperature limit, and, at zero field, the dispersion relation  $E_{\vec{q}}$  for the triply degenerated dimer excitations is given by

$$E_{\vec{q}}^2 = (\Delta + 2\lambda_1) \left( \Delta + 2\lambda_1 - \frac{2}{1 + 4\lambda_2} [J(\vec{q}) - 2\lambda_1] \right). \quad (5)$$

$\Delta = J_0$  is the singlet-triplet energy gap for the noninteracting dimers, and the expressions for the parameters  $\lambda_1$  and  $\lambda_2$  are given in Ref. [14]. This dispersion relation is equivalent to the RPA result with effective values for the interacting

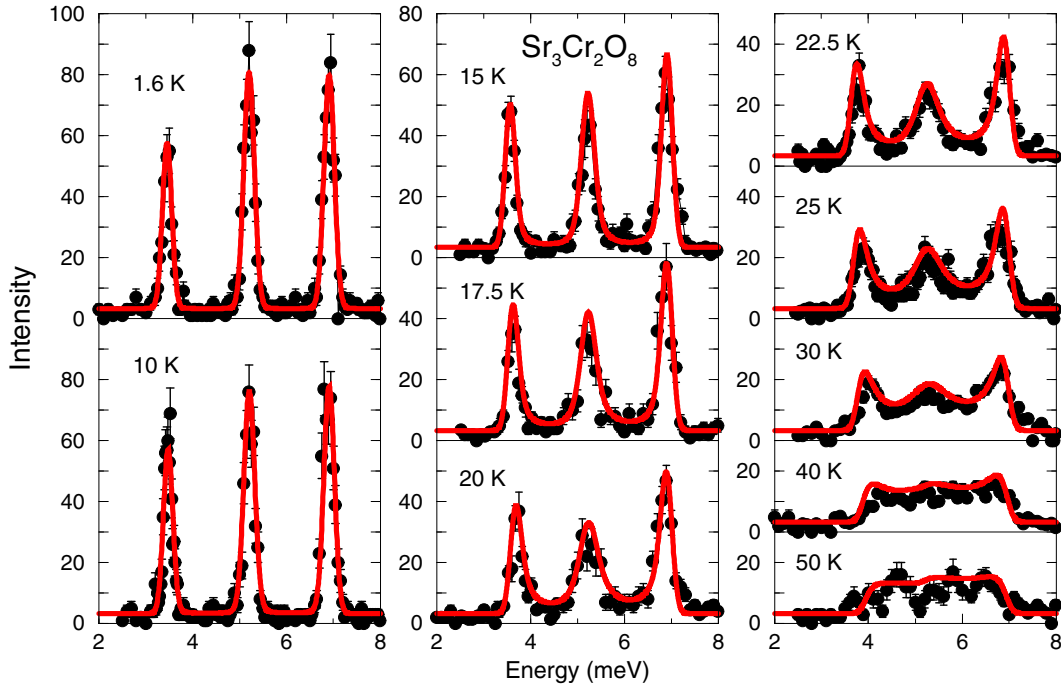


FIG. 2. (Color online) Constant  $Q$  scans at  $(0.5, 0.5, 3)$  measured at different temperatures on V2-FLEX. The solid lines are the calculated response functions assuming the fitted experimental resolution function to be independent of temperature. The three peaks derive from the three equivalent crystallographic twins.

parameters:  $E_{\vec{q}}^2 = \Delta_{\text{eff}}[\Delta_{\text{eff}} - 2J_{\text{eff}}(\vec{q})]$ . The RPA analysis of the excitation spectrum measured at 1.6 K shows that  $\Delta_{\text{eff}} = 5.551$  meV [2,3], and using the exchange parameters given by Table II in Ref. [3] the density of states becomes the one shown in Fig. 1, when averaging the results for the three twinned domains. From this density of states the self-consistently derived parameters are  $\lambda_1 = 0.05134$  meV and  $\lambda_2 = 0.004885$ , and thereby  $\Delta_{\text{eff}} = 1.0378\Delta$  and  $J_{\text{eff}}(\vec{q}) = 0.9632J(\vec{q})$ .

#### IV. THEORY IN COMPARISON WITH EXPERIMENTS

The single-site Green's functions  $G_p(i\omega_n)$ , which determine the correlation functions for the singlet-triplet system to first order in  $1/z$ , were derived in Ref. [14]. Using the exchange parameters determined experimentally in terms of the effective RPA model, i.e., the density of states shown in Fig. 1, there are no free parameters left in the theory.

Figure 2 shows a comprehensive comparison between experiments and theory for the spin dynamics in  $\text{Sr}_3\text{Cr}_2\text{O}_8$ . The three magnetic excitations observed at the wave vector  $(0.5, 0.5, 3)$  (r.l.u.) cover the whole band of excitations. One of the peaks lies in the middle of the band at an energy close to  $\Delta$ , whereas the lower (upper) peak derives from an excitation at the lower (upper) boundary of the excitation band. The experimental resolution function is assumed to be the same at all temperatures and to be resolved by the three peaks at 1.6 K. Assuming a small constant background, these three peaks were fitted by three Gaussians independently of each other, i.e., the width and scale factor are allowed to depend on frequency. The excitation energies were also modified slightly in comparison with that predicted by the RPA model at this wave vector. The

comparison in Fig. 2 shows that the theory accounts accurately for all the different modifications of the spectrum that develop as the temperature is increased. In comparison with the RPA theory (see Refs. [2,3]), the present theory predicts about the same decrease in intensities, but the agreement between the experimental and theoretical reductions of the bandwidth has been improved significantly. Most importantly, the theory in the order  $1/z$  now predicts a finite lifetime of the excitations at nonzero temperatures.

Although the scattering intensities from the three excitations overlap each other appreciably above 25 K, there is no doubt that the theory is close to predicting the right lineshapes of the three peaks all the way up to 50 K. The

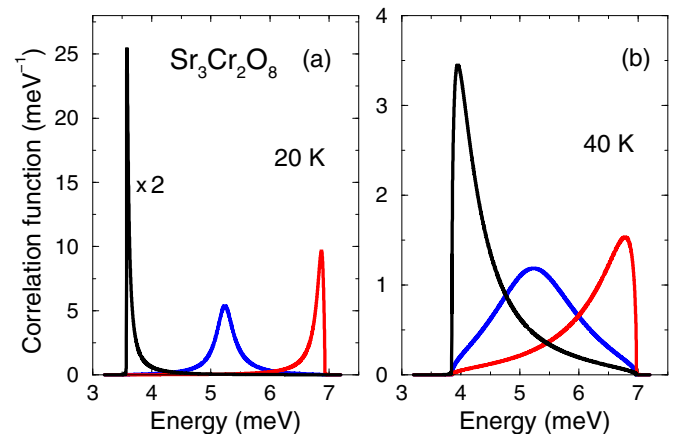


FIG. 3. (Color online) The intrinsic shapes of each of the three peaks considered in Fig. 2 calculated at (a) 20 and (b) 40 K. The correlation function corresponding to the peak at the lowest energy has been divided by two in (a).

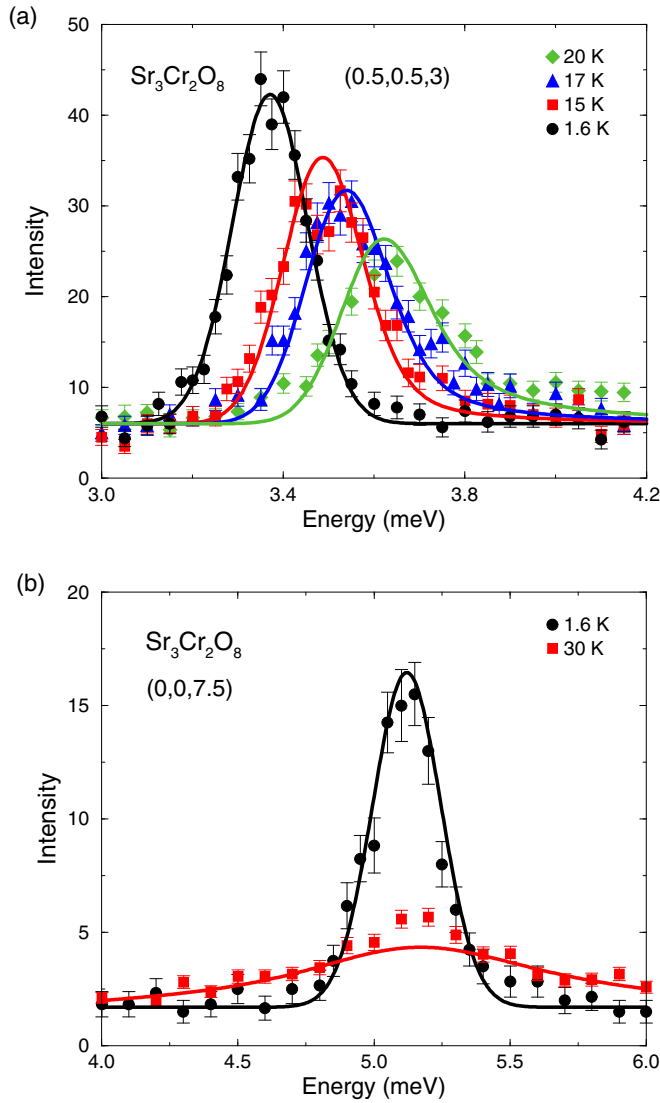


FIG. 4. (Color online) Constant  $Q$  scans performed at TASP. The temperature variation of the low energy peak at  $(0.5, 0.5, 3)$  is shown in (a), and of the single excitation at  $(0, 0, 7.5)$  in (b). The solid lines are the calculated response functions using experimental resolution functions determined by the scans at 1.6 K.

separate scattering functions (without resolution convolution) corresponding to each of the three peaks at  $(0.5, 0.5, 3)$  in Fig. 2 at 20 and 40 K are shown in Fig. 3. An analysis of the complex expressions derived for Green's functions in Ref. [14] to first order in  $1/z$  shows that the lineshapes are determined by a Lorentzian-like function with a frequency dependent width (see also the discussion of the singlet-singlet case in Ref. [1]). This width is proportional, mainly, to a temperature-dependent factor  $n_0 + n_1 - (n_0 - n_1)^2$  and to the frequency-dependent density of states of the excitations. Here  $n_0$  and  $n_1$  are the population numbers of, respectively, the ground state and one of the excited triplet states within the MF approximation. To first order in  $1/z$ , the lineshape for a certain excitation depends only on its energy, not on its wave vector; hence Fig. 3 is representative for most theoretical possibilities. The scattering intensities vanish at energies outside the excitation

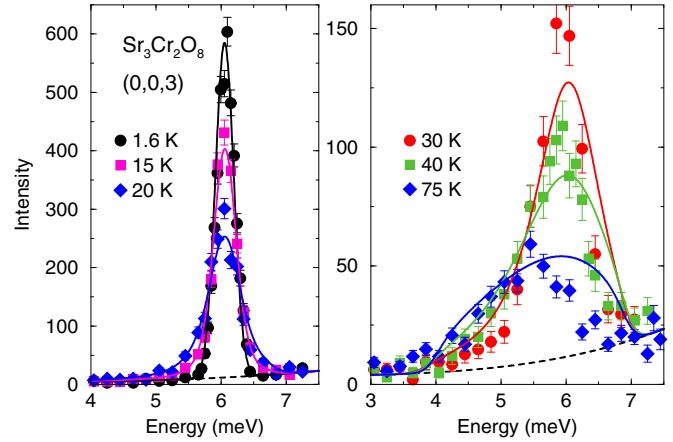


FIG. 5. (Color online) Constant  $Q$  scan at  $(0, 0, 3)$  measured at different temperatures on V2-FLEX. The solid lines are the calculated response functions assuming the smooth but nonlinear background indicated by the dashed line.

band. Consequently, the lineshape of an excitation close to the upper or the lower edge becomes strongly asymmetric because of the cutoff at the band edge, whereas the lineshape for an excitation in the middle of the band is close to being symmetric.

The more narrow experimental resolution used at TASP, due to tighter collimation and lower selected final wave vector, has been utilized for a closer examination of the low energy peak at  $(0.5, 0.5, 3)$  as shown in Fig. 4(a). In addition, the single-excitation case at  $(0, 0, 7.5)$  was studied leading to the results shown in Fig. 4(b); here the excitation energy lies close to the center of the band as for the middle excitation in Fig. 2. The slight deviation between theory and experiment in Fig. 4(a) at the upper tail of the  $(0.5, 0.5, 3)$  peak at 20 K derives mostly from the lower tail of the scattering peak at about 5 meV, which starts to overlap at this temperature, but which is not included in the calculated scattering function. Once again the theory accounts nearly perfectly for the temperature dependencies of the scattering peaks. The only minor discrepancy detected is that the maximum intensity of the  $(0, 0, 7.5)$  peak at 30 K seems to be slightly larger than predicted.

Finally, the single excitation at  $(0, 0, 3)$  was examined within a broad range of temperatures using the V2-FLEX spectrometer. The experimental results compared with the theoretical ones are shown in Fig. 5. Once again the experimental data at 1.6 K have been used for determining the experimental resolution function. Unfortunately, the background is not constant in this case, due to the small scattering angle at the analyzer giving a weak contamination from the direct beam. The data at 1.6 K show a clear increase of the background when going from 6.5 to 7 meV, but it is impossible to decide whether there is a smooth increase of the background in the interval from 5 to 7.5 meV, as assumed in Fig. 5, or whether there is a more sharp increase around 6.5 to 7 meV. The latter assumption would lead to a substantial improvement of the comparison between experiments and theory in this figure. In all circumstances, the comparison indicates that the scattering from the present excitation is slightly more narrow and the energy slightly smaller than predicted for temperatures

greater than half the corresponding averaged excitation energy (i.e., for  $T \geq \Delta/2k \approx 30$  K).

## V. CONCLUSION

The critical ratio between the exchange coupling of different dimers and the intradimer interaction in  $\text{Sr}_3\text{Cr}_2\text{O}_8$  is about 63% of that required for inducing an antiferromagnetically ordered state at zero field and temperature. It would require an applied magnetic field of about 29 T to force the system to order at zero temperature, but although the exchange interaction between the dimers is too weak to induce order by itself, the singlet-triplet excitations are strongly dispersive, collective modes.

The damping of bosonic excitations like spin waves (in systems with large  $S$ ) only appears in the second order of  $1/z$  [9], and the excitations of these systems are typically observed to have a symmetric Lorentzian lineshape. In contrast, the magnetic excitations deriving from a single excited level at the local sites are damped to first order in the high-density  $1/z$  expansion [8]. The first-order damping appears because the collective excitations are not able to propagate via sites which are already in an excited state. This hard-core constraint leads to asymmetries in the lineshapes deriving from variations in the density of excited states. In the case of the present system, the first-order theory, developed originally for the equivalent dimer system  $\text{TlCuCl}_3$  [14], leads to an accurate description of the excitations in  $\text{Sr}_3\text{Cr}_2\text{O}_8$  over a nearly complete range of energies and temperatures. There are some discrepancies between experiment and theory for the excitation at the wave vector  $(0,0,3)$ , but considering the good agreement obtained in all other cases, we think that a major part of these discrepancies relate to our ignorance of the background here. The present  $1/z$  theory involves a self-consistently determined “effective fluctuating medium.” This further development of the theory is important, not least for the calculated shapes of the scattering peaks, since the original, unconditional theory by Stinchcombe predicts a substantial narrowing of the excitations with energies close to  $\Delta$  in disagreement with experiments (see the discussion in Refs. [1,11]).

The effective-medium  $1/z$  theory for a singlet-triplet system gives also a satisfactory account for the behavior of the excitations observed in the case of  $\text{TlCuCl}_3$  [19], although the possibility of an asymmetric thermal lineshape broadening was not considered in Ref. [19]. In addition, the theory is found to offer a reliable estimate of the modifications of the macroscopic MF properties of this system [14]. The same holds true for the singlet-singlet systems  $\text{HoF}_3$  [11,20] and  $\text{LiHoF}_4$  [12]. In particular, the phase diagram predicted for  $\text{LiHoF}_4$ , an Ising magnet in a transverse field, is found to be nearly identical with that determined by a quantum Monte Carlo calculation [21,22].

The expansion to first order in  $1/z$  appears to be sufficiently accurate for the present comparisons between experiments and theory. The second-order contributions to the single-site Green’s function have been considered in the case of elemental praseodymium metal, where the critical ratio is about 0.92 [13]. The second order terms give rise to two fundamental modifications, the line widths stay nonzero in the zero temperature limit, and the scattering intensities become nonzero also outside the excitation band determined to first order in  $1/z$ . However, both modifications turned out to be of only marginal importance in the case of Pr metal.

We may conclude that  $\text{Sr}_3\text{Cr}_2\text{O}_8$  can be added to the list of strongly correlated systems, where the diagrammatic high-density expansion to first order in  $1/z$  leads to an accurate description of the properties of the ground state and the excitations, when applying the effective-medium approach. The success of this theory is not accidental, and its ability to capture the hallmarks of strong correlations, such as asymmetric thermal lineshape broadening, proves that it deserves more attention than given to it hitherto.

## ACKNOWLEDGMENTS

The authors would like to thank Henrik Smith and Christian Rüegg for stimulating discussions. This work is partially based on experiments performed at the Swiss spallation neutron source SINQ, Paul Scherrer Institute, Villigen, Switzerland.

- 
- [1] J. Jensen and A. R. Mackintosh, *Rare Earth Magnetism: Structures and Excitations* (Clarendon Press, Oxford, 1991), <http://www.nbi.ku.dk/page40667.htm>
  - [2] D. L. Quintero-Castro, B. Lake, A. T. M. N. Islam, E. M. Wheeler, C. Balz, M. Månsson, K. C. Rule, S. Gvasaliya, and A. Zheludev, *Phys. Rev. Lett.* **109**, 127206 (2012).
  - [3] D. L. Quintero-Castro, B. Lake, E. M. Wheeler, A. T. M. N. Islam, T. Guidi, K. C. Rule, Z. Izaola, M. Russina, K. Kiefer, and Y. Skourski, *Phys. Rev. B* **81**, 014415 (2010).
  - [4] D. A. Tennant, B. Lake, A. J. A. James, F. H. L. Essler, S. Notbohm, H.-J. Mikeska, J. Fielden, P. Kögerler, P. C. Canfield, and M. T. F. Telling, *Phys. Rev. B* **85**, 014402 (2012).
  - [5] F. Groitl, K. Habicht, K. Rolfs, T. Keller, and D. Alan Tennant (unpublished).
  - [6] G. Misguich and M. Oshikawa, *J. Phys. Soc. Jpn.* **73**, 3429 (2004).
  - [7] J. Sirker, A. Weisse, and O. P. Sushkov, *J. Phys. Soc. Jpn. Suppl.* **74**, 129 (2005).
  - [8] R. B. Stinchcombe, *J. Phys. C: Solid State Phys.* **6**, 2459 (1973); **6**, 2484 (1973); **6**, 2507 (1973).
  - [9] V. G. Varks, A. I. Larkin, and S. A. Pikin, *Zh. Eksp. Teor. Fiz.* **53**, 1089 (1968) [*Sov. Phys. JETP* **26**, 647 (1968)].
  - [10] J. Jensen, *J. Phys. C: Solid State Phys.* **17**, 5367 (1984).
  - [11] J. Jensen, *Phys. Rev. B* **49**, 11833 (1994).
  - [12] H. M. Rønnow, J. Jensen, R. Parthasarathy, G. Aeppli, T. F. Rosenbaum, D. F. McMorrow, and C. Kraemer, *Phys. Rev. B* **75**, 054426 (2007); H. M. Rønnow, R. Parthasarathy, J. Jensen, G. Aeppli, T. F. Rosenbaum, and D. F. McMorrow, *Science* **308**, 389 (2005).

- [13] K. A. McEwen, U. Steigenberger, and J. Jensen, *Phys. Rev. B* **43**, 3298 (1991).
- [14] J. Jensen, *Phys. Rev. B* **83**, 064420 (2011).
- [15] L. C. Chapon, C. Stock, P. G. Radaelli, and C. Martin, [arXiv:0807.0877](https://arxiv.org/abs/0807.0877) [cond-mat.mtrl-sci].
- [16] Z. Wang, M. Schmidt, A. Günther, S. Schaile, N. Pascher, F. Mayr, Y. Goncharov, D. L. Quintero-Castro, A. T. M. N. Islam, B. Lake, H.-A. Krug von Nidda, A. Loidl, and J. Deisenhofer, *Phys. Rev. B* **83**, 201102(R) (2011).
- [17] D. Wulferding, P. Lemmens, K.-Y. Choi, V. Gnezdilov, Y. G. Pashkevich, J. Deisenhofer, D. Quintero-Castro, A. T. M. N. Islam, and B. Lake, *Phys. Rev. B* **84**, 064419 (2011).
- [18] A. T. M. N. Islam, D. L. Quintero-Castro, B. Lake, K. Siemensmeyer, K. Kiefer, Y. Skourski, and T. Herrmannsdorfer, *Cryst. Growth Des.* **10**, 465 (2010).
- [19] Ch. Rüegg, B. Normand, M. Matsumoto, Ch. Niedermayer, A. Furrer, K. W. Krämer, H.-U. Güdel, Ph. Bourges, Y. Sidis, and H. Mutka, *Phys. Rev. Lett.* **95**, 267201 (2005).
- [20] A. P. Ramirez and J. Jensen, *J. Phys.: Condens. Matter* **6**, L215 (1994).
- [21] S. M. A. Tabei, M. J. P. Gingras, Y.-J. Kao, and T. Yavors'kii, *Phys. Rev. B* **78**, 184408 (2008).
- [22] The close agreement between the two theories was not realized by Tabei *et al.* [21], and their article also contains several misunderstandings of the analysis presented in Ref. [12].